Permeation of Hairless Mouse Skin II: Membrane Sectioning Techniques and Influence on Alkanol Permeabilities

G. L. FLYNN ˣ, H. DÜRRHEIM, and W. I. HIGUCHI

Received September 1, 1979, from the *College of Pharmacy, University of Michigan, Ann Arbor, MI 48109.* Accepted for publication July 17, 1980.

Abstract □ The barrier properties of hairless mouse skin were examined by separating the skin into its component epidermal and dermal strata, using both mechanical and thermal techniques, and then assessing the permeability of each stratum to the homologous alkanols. The permeability data, when compared to those obtained previously for full-thickness hairless mouse skin and to new data for the permeability of the alcohols through a perfect lipid membrane, allow assignment of diffusional resistances to the respective, anatomically distinguishable membrane strata. It was found that the principal barrier for the lower alkanols is the epidermis, which contains the stratum corneum. The effective aqueous tissue resistances of the cellular and aqueous strata of full skin, the epidermis, and the dermis were estimated using sectioned skins. This resistance was much greater than that of an equivalent thickness of water. These data and methods represent a novel approach in the permeation analysis of a biological tissue and offer a means of estimating the effects of skin damage on percutaneous absorption.

Keyphrases □ Permeability—*n*-alkanols through hairless mouse skin strata separated by thermal and stripping techniques □ Alcohols, normal—permeation through hairless mouse skin strata separated by thermal and stripping techniques □ Skin separation techniques—separation of hairless mouse skin strata by thermal and stripping techniques, permeability of *n*-alkanols through separated strata

The skins of mammals differ widely in appearance and function (1). Even the skins of animals without prominent, terminal hair vary greatly, but all have a more fully developed epidermis with a significant outer horny or cornified layer, which functions protectively in the absence of hair. Human and hairless mouse integuments are two examples of such skins.

Cornified epithelia are unusually impermeable to both inorganic and organic chemicals (2–4). This feature of human skin limits the topical use of drugs but, at the same time, protects the body from inadvertently encountered toxins in the environment and in products of everyday use. Clearly, the delineation of barrier features and the construction of predictive models are important steps in defining topical usefulness and the risk of chemicals.

Ideally, models should be so refined that quantitative *a priori* estimates of percutaneous absorption rates based on chemical structure are possible. Some beginnings have been made in this regard (5–7), but it still is not possible to predict the permeability of a new compound unless it is related congenerically to previously studied chemicals. Furthermore, the influences of injury and disease are poorly documented. Laboratory means of assessing the effects of trauma have yet to be developed.

The purpose of the present study was to assess the permeabilities of hairless mouse skin strata, isolated by thermal and stripping techniques. Water and homologous alkanols were chosen as the permeants. By defining the diffusional resistances of each layer, especially the stratum corneum, as a function of the alkyl chain length, it should be possible to learn generally how systemic absorption as a result of stratum corneum impairment is related to the chemical structure of permeants. Gross similarities in permeability properties between hairless mouse skin and human skin make the insights relevant to humans. In this sense, the techniques developed may prove to be useful as laboratory methods for defining maximum absorption potentials and, therefore, maximum systemic toxicities of topically applied chemicals and drugs.

EXPERIMENTAL

The present study represents a continuation of research on alkanol permeation of hairless mouse skin, for which experimental methods were described (5). The description of the experimentation details only departures from previous methods. Chemical sources, diffusion cell design and operation, and partitioning techniques also were the same as those reported previously (5).

The abdominal skins of hairless mice (HRS/J strain), 4–6 weeks old, were excised and used essentially upon receipt. The skin either was used intact or was separated into its respective strata by one of the following methods.

1. Heat treatment—The skin was separated along the epidermal–dermal junction after the abdominal surface of an anesthetized (methoxyflurane[1]) mouse was heated for 30 sec with a stream of 60° water. The animals were sacrificed, and the heat-treated skin was excised intact and separated carefully into the epidermis and dermis by raising the epidermal layer with the sharp end of a nickel spatula. Each stratum then was placed in a separate diffusion cell. The heat-separated epidermis was laid gently on the surface of normal saline solution to flatten and smooth it. This step caused the layer to unwrinkle spontaneously so that it could be lifted and placed between the cell halves if handled carefully.

2. Stripping technique—The hairless mouse skin was stripped repeatedly with cellophane tape[2]. The tape was placed firmly against the abdominal surface of an anesthetized mouse and then peeled away. This procedure was done in multiples of five strippings for up to 15 strippings and was carried out 25 times on some skins. The skin became more and more an oozing surface with each succeeding maneuver. After processing the skin, the animal was sacrificed and the skin was excised and mounted in the diffusional apparatus. The processing of the mouse skin is illustrated schematically in Fig. 1.

After positioning of the membrane in the diffusion cell, the apparatus was immersed in a 37° bath, the cell compartments were rinsed with normal saline, and the runs were conducted at 150 rpm (2). To assess boundary layer influences, polydimethylsiloxane membranes[3] were used since they provide a simple, hydrophobic membrane without internal aqueous resistance. Therefore, departure from membrane-controlled transport could be assigned totally to hydrodynamic layers at the membrane interfaces with the compartmental solutions (8, 9). The preparation of the diffusion cell after insertion of the rubber membrane was identical to that used for the skin membranes.

The permeation process, irrespective of the membrane, was tracked using radiolabeled alcohols. The permeability coefficient for each run was calculated from the pseudo-steady-state portion of the receptor compartment concentration *versus* time profile using (5):

$$P = V_R \left(\frac{dC/dt}{A\,\Delta C} \right) \qquad \text{(Eq. 1)}$$

[1] Metophase, Pitman–Moore, Washington Crossing, NJ 08560.
[2] Scotch Brand, 3M Co., Minneapolis, Minn.
[3] Silastic medical grade sheeting, 0.05 cm, Dow Corning Corp., Midland, Mich.

0022-3549/81/0100-0052$01.00/0

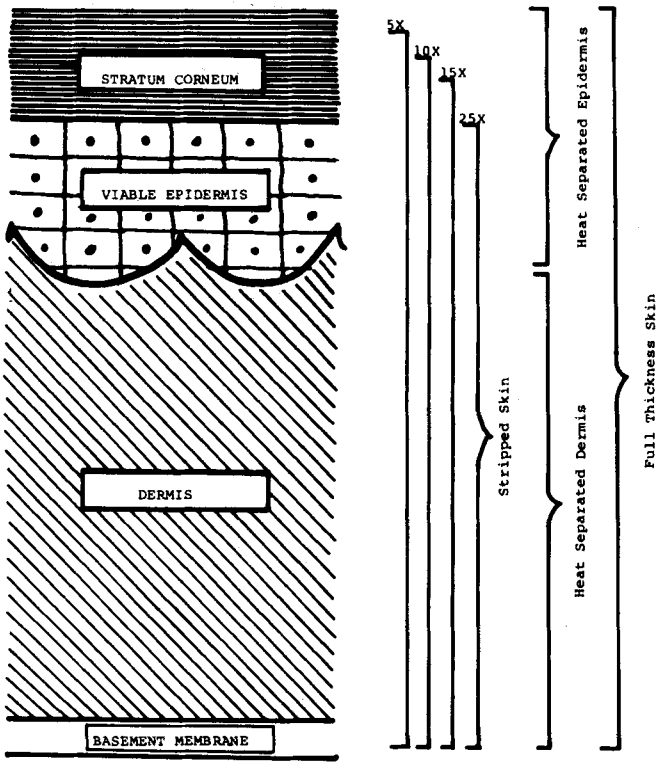

Figure 1—*Schematic diagram of the skin indicating the consequences of the various fractionation techniques on the processed membrane compositions. This diagram represents the structure of the mouse skin based on gross visual examination, on its physicochemical behavior as seen in permeability experiments, and on traverse histological sections viewed under the light microscope. Residuals of hair follicles seen in traverse sections are not represented.*

where V_R is the receiver volume, dC/dt is the steady-state rate of change in the receiver concentration (counts per minute), A is the exposed cross-sectional area of the membrane, and ΔC is the concentration (counts) differential between compartments. The value of ΔC effectively is the donor concentration (counts) since the buildup of material in the receiver was never allowed to become a significant fraction of that in the donor compartment. Except as indicated, the data represent single determinations.

Some partitioning work also was done on both processed skins and the synthetic membrane. Procedural details and the method of calculation were presented previously (5).

RESULTS AND DISCUSSION

The data for partitioning of the alcohols into full-thickness hairless mouse skin, hairless mouse epidermis, and the polydimethylsiloxane membrane from saline solution[4] are summarized in Table I. The full-thickness skin and silicone rubber membrane data are presented in Fig. 2, where the partition coefficients are plotted semilogarithmically against the alkyl chain length. Polydimethylsiloxane partitioning followed an exponential trend through the entire series, while the partitioning dependency for the tissue was biphasic. The silicone rubber dependency followed the form:

$$\log K_n = \log K_0 + \pi n \qquad \text{(Eq. 2)}$$

where K_n is the partition coefficient of the homolog of chain length n, $\log K_0$ is the intercept of the plot on the y-axis corresponding to the partitioning of the hypothetical zero chain length homolog, and π is the incremental increase in the logarithm of the partition coefficient per methylene unit. The least-squares values for these parameters are π = 0.417 and K_0 = 0.029, with a correlation coefficient of 0.998. The trend predicted by Eq. 2 is the expected behavior for alkyl homologs (10–13),

[4] Sodium Chloride Irrigation (0.9%), Abbott Laboratories, North Chicago, IL 60064.

Table I—Partitioning[a] of the Alkanols between 0.9% Saline and Full-Thickness Skin, Epidermis, and Silicone Rubber

Alkanol	Full-Thickness Skin[a]	Heat-Separated Epidermis[a]	Polydimethylsiloxane[a,b]
Methanol	5.5	—	0.064
Ethanol	5.4	4.5	0.256
n-Propanol	6.0	4.4	0.612
n-Butanol	6.6	5.3	1.18
n-Pentanol	7.7	5.1	2.85
n-Hexanol	10.7	14.0	11.0
n-Heptanol	24.0	24.1	23.0
n-Octanol	40.8	68.5	57.7
n-Nonanol	86.7	118	194
n-Decanol	—	—	412

[a] The data are in grams per cubic centimeter. For silicone rubber, the K values can be considered as unitless since the density of commercial polydimethylsiloxane is close to unity. [b] The slope of these data on a log K *versus* alkyl chain length plot is 0.417 (r = 0.998).

but the magnitude of the slope (π value) is less than that found previously for partitioning between silicone rubber and water for a different homologous series, the alkyl *p*-aminobenzoates (0.54) (8). Based on work to be reported separately, this difference in estimates of π appears to be related largely to differences in intermolecular interactions in the polymeric phase.

The partitioning data for the epidermis indicate that it is a two or more phase structure physicochemically, with lower alcohols exhibiting no alkyl chain length dependency but with higher homologs evidencing a marked, exponential acclivity. The same behavior was observed with the full-thickness skin. The preliminary indications are that the polar compounds

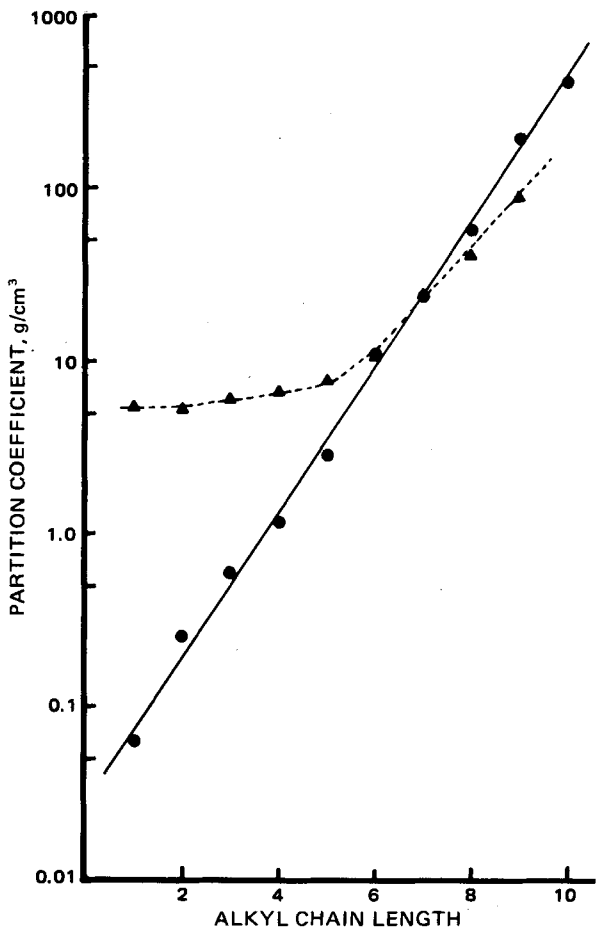

Figure 2—*Semilog plot of membrane–saline partition coefficients against alkyl chain length for polydimethylsiloxane (●) and for full-thickness skin (▲). The π value (slope) for silicone rubber is 0.417. The data for the skin are biphasic with a terminal acclivity (C_6–C_9) of 0.296.*

Table II—Permeability Data for Commercial Polydimethylsiloxane Membranes[a] at 37°

Alkanol	$P_n \times 10^3$, cm/hr	$D_n \times 10^6$, cm²/sec
Methanol	6.8	1.49
Ethanol	33.5	—
n-Propanol	28.8	0.66
n-Butanol	56.6	0.68
n-Pentanol	123.2	0.61
n-Hexanol	301	0.39
n-Heptanol	339[b]	—
n-Octanol	335[b]	—
n-Nonanol	303[b]	—
n-Decanol	315[b]	—

[a] Silastic medical grade sheeting, Dow Corning, Midland, Mich. [b] These data are apparent values affected by membrane retention of the alkanols in the quasi-steady state and deviate significantly from expected values for a true steady state.

concentrate in the aqueous compartments of the tissue but that the nonpolar regions become the principal areas of accumulation as the compounds become more hydrophobic. The similarity between epidermal and full-thickness skin values likely means that the consequential nonpolar phase is common to both tissues.

Permeability coefficients for polydimethylsiloxane membranes are presented in Table II. These values evidence an exponential increase up to a chain length of about seven and then level off at a permeability coefficient of slightly over 0.3 cm/hr. Neglecting ethanol, which for reasons unknown does not conform to the trend[5], the exponential dependency of the C_1–C_6 data yields a value of 0.326 for π ($r = 0.999$), which is somewhat less than the partitioning π value. This difference in the π value is not entirely unexpected since the permeability coefficient under membrane control is dependent on diffusivity as well as on the partition coefficient. The diffusion coefficient values for the homologs in the silicone rubber matrix decrease with increasing molecular size, which would impact on the π constant evaluated from permeabilities in the observed fashion. Diffusivities (D_n) are listed in Table II for methanol through *n*-hexanol, except for ethanol. These valves were calculated from the following relationship, which assumes that the membrane is the rate-controlling barrier acting as an isotropic phase:

$$D_n = \frac{P_n h_M}{3600 K_n} \qquad \text{(Eq. 3)}$$

where D_n, P_n, and K_n designate the diffusivity in square centimeters per second, the permeability coefficient in centimeters per hour, and the partition coefficient of the *n*th chain length compound, respectively, and h_M is the thickness of the membrane. The factor 3600 converts the diffusion coefficient to the more conventional units of reciprocal seconds. Since the density of silicone rubber is close to one, little error is introduced in using the partition coefficients as reported, that is, in units of grams per cubic centimeter. The magnitudes of the polydimethylsiloxane diffusivities reported, $\sim 10^{-6}$ cm²/sec, are entirely reasonable.

The plateau in the permeation of polydimethylsiloxane past hexanol at first suggests the onset of boundary layer control. However, the effective boundary layer thickness based on an aqueous diffusivity for the alkanols at 37° of 1×10^{-5} cm²/sec and a permeability coefficient of ~0.3 cm/hr is 1200 μm, which seems to be unreasonably large by a factor of three to four. Examination of the donor compartment depletion side by side with the receiver accumulation revealed that, above a chain length of six, only fractional amounts of the material entering the membrane were exiting from the other side in the pseudo-steady state.

Application of the pseudo-steady-state procedure to obtain fundamental permeation constants is based on the assumption of insignificant membrane retention of the diffusing compound during the experiments (12, 14). This condition is not achieved above a chain length of six in the polydimethylsiloxane studies due to the exponentially increasing membrane–water partition coefficient and the small volumes (1.5 ml) of the cell compartments. The capacity of the membrane for octanol relative to the aqueous phases, which is the product of its partition coefficient (57.7) and the membrane volume (0.0508-cm thickness times an area of ~0.7 cm² ≃ 0.035 cm³), is 2.0 ml, which is greater than the capacity of one of the aqueous compartments; thus, significant percentages

[5] This data point was repeated several times and always gave the same apparently high result. However, in later studies by C. R. Behl using a different lot of radiolabeled ethanol, a value of 16 was obtained, which is more consistent with the overall trend.

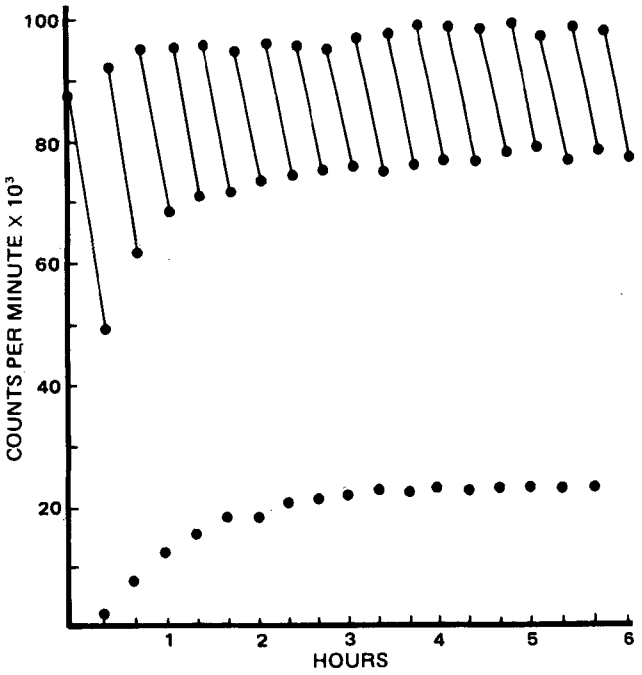

Figure 3—*Experimental data from the exchange procedure for* n-*octanol permeating the polydimethylsiloxane membrane at 37°. The plot is expressed in counts per minute at the beginning and end of each 20-min interval (each pair connected with a line) for the donor phase and counts per minute in the receiver at the end of each interval. It is notable that it takes about 3 hr (nine exchanges) before a steady state (plateau) is reached.*

of the higher alkanols ($n \geq 8$) remain within the membrane.

To estimate the permeability value for *n*-octanol validly and to determine the actual boundary layer effect, a procedure was developed that involved totally changing the donor and receiver cell compartment contents at fixed sampling intervals of 20 min. The donor was replaced repeatedly with a solution of the initial concentration, and the receiver was exchanged with fresh saline. This process was done in lieu of using very large compartmental volumes, which also would have neutralized the membrane retention influences, since the purpose was to assess the permeability coefficient under the same hydrodynamic conditions used for the lower alkanols.

Data for the exchange procedure are displayed in Fig. 3. The amounts (counts) in the donor compartment at the beginning and end of each interval and the amounts (counts) in the receiver at each interval termination are plotted against time. The bars on the upper set of data (donor data) join the data points for the front and back ends of a given interval. Both the upper and lower linked sets of points increase systematically to an asymptotic value, but the gap narrows to ~20,000 cpm.

Table III—Permeability Data for Heat-Treated Skin

	$P_n \times 10^3$, cm/hr			
Alkanol	Full-Thickness Skin	Full-Thickness[a] Skin, Heat Treated	Heat-Separated[a] Epidermis	Heat-Separated[a] Dermis
Methanol	2.6 (0.46)[b]	—	2.3	318
Ethanol	4.8 (0.43)	3.91	4.7	303
n-Propanol	5.4	—	9.7	289
n-Butanol	14.6 (0.81)	16.2	16.8	287
n-Pentanol	22.0	39.4	29.3	285
n-Hexanol	48.0 (1.2)	—	58.5	266[c]
n-Heptanol	92.9	157	113	246
n-Octanol	97.2[d] (2.4)	153[d]	180[d]	204[d]
n-Nonanol	88.8[d]	164[d]	248[d]	93[d]
n-Decanol	84.5[d]	—	233[d]	90[d]

[a] These results are single determinations. [b] Standard deviations of multiple runs. [c] Interpolated value. [d] These data points may be affected by membrane retention and, therefore, represent apparent P values under the conditions of the experiment.

Table IV—Estimation of the Resistance of Hairless Mouse Skin Strata for the Lower Alkanols

Alkanol	Resistance[a], hr/cm				Total Aqueous Resistance[c], %
	R_{aq}	R_{sc}	R_{vt}	R_{total}[b]	
Methanol	0.83	382	2.31	385	0.82
Ethanol	0.83	205	2.47	208	1.6
n-Propanol	0.83	182	2.63	185	1.9
n-Butanol	0.83	65	2.65	68.5	5.1
n-Pentanol	0.83	42	2.68	45.5	7.7
n-Hexanol	0.83	17	2.93	20.8	18.1

[a] Generally, $R = h/DK$ for an isotropic phase, where h is the thickness, D is the diffusion coefficient, and K is the partition coefficient with respect to the donor compartment solution. [b] Total resistance = $1/P_n = R_{aqI} + R_{sc} + R_{vt} + R_{aqII}$, where R_{aqI} and R_{aqII} are the boundary layer resistances, R_{vt} is the viable tissue resistance, and R_{sc} is the resistance encountered in the stratum corneum. The individual resistances are obtained by difference. [c] Total aqueous resistance is $R_{aq} + R_{vt}$ (sum of the boundary layer and viable tissue resistances).

This plot indicates initial rapid membrane loading that tapers off appreciably with each succeeding interval. The receiver data demonstrate that little material diffuses across the membrane in the earliest intervals as the membrane gradient is formed; but as the membrane becomes loaded, the receiver accumulation in an interval also increases to a plateau of ~20,000 cpm.

When the amount leaving the donor compartment comes into coincidence with the amount entering the receiver, the process is effectively in a true steady state and the permeability coefficient can be calculated from either the donor or receiver data. This conclusion was reached both through computer-assisted analysis of a rigorous mathematical model written for the exchange procedure and through extensive additional experimentation, both of which were reported separately (15, 16). The permeability coefficient for octanol exceeds 1.0 cm/hr and is close to the extrapolation of the exponential trend seen for lower homologs, meaning that the permeation of octanol is substantially membrane controlled. Thus, in this diffusional system operated at a 150-rpm stirring rate, the aqueous boundary layers have a collective effective thickness of <350 μm[6]. The thickness is estimated from the permeability coefficient and from the boundary layer control relationship:

$$P = \frac{D_{AQ}}{\Sigma h_{AQ}} \qquad \text{(Eq. 4)}$$

where D_{AQ} is the aqueous diffusivity ($\simeq 1 \times 10^{-5}$ cm^2/sec) and Σh_{AQ} is the total thickness of the unstirred layers. In the following analysis, a boundary layer resistance of 0.83 cm/hr, equivalent to a thickness for the hydrodynamic layers of 300 μm, is assumed. Little error is introduced using this value, even if it is inexact, since it is small and a relatively insignificant fraction of the total aqueous resistance encountered in the skin membranes.

Permeability coefficients obtained for the alkanols at 37° for full-thickness skin, heat-separated epidermis and dermis, and full-thickness skin scalded for 30 sec at 60° but not fractionated are given in Table III. These data also form the basis for Fig. 4, in which the log of the permeability coefficient is plotted against alkyl chain length. No extreme effect on permeability was produced by scalding 60° water applied to the skin for 30 sec, a treatment that was estimated to give a deep partial-thickness to full-thickness burn. When burned full-thickness skin data are compared with similar data on untreated skin, no more than a twofold increase in permeability is noted for any homolog; for ethanol and butanol, the values are not different within experimental uncertainty.

When the heat-separated epidermal data are considered side by side with the full-thickness normal and burned skin data, a striking similarity in the permeabilities for the lower homologs ($n < 8$) is seen. In all of these cases, the stratum corneum is intact, and considering all of the data, it appears to be the principal source of diffusional resistance for the polar compounds. Data on the epidermis support the observation that scalding the skin as described has no profound effect, although somewhat higher permeability coefficients for the middle homologs consistently are noted. This observation is important since the heat-separation technique has been commonly used to prepare human skin membranes for diffusional studies (17–19).

[6] Based on extensive experimental work beyond that reported here, the diffusion layers appear to be ~300 μm in total thickness (15, 16).

Considering only the full-thickness skin and epidermis, it appears as if the removal of the thick dermal matrix leads to increased permeation rates at long alkyl chain lengths, which suggests that the dermis acts as an aqueous matrix. This conclusion is somewhat tenuous, because membrane retention was not factored out of these data. By actual measurement, the epidermis is only 40 μm thick, which minimizes such concern in its case. However, the total skin is about 10 times thicker and, therefore, amounts to a significant compartment for the higher partitioning, nonpolar homologs. The data are meaningful even with the membrane retention influence included since retention would be encountered on topical application and thereby influence the quantities percutaneously absorbed. A further general conclusion is that the composite mouse tissue behaves almost identically to the excised skin of human, as evidenced in the collective studies of Scheuplein and associates (17–19).

Comparison of the heat-separated dermis data with the data for normal skin reveals that the barrier is compromised severely when the epidermis is removed. Moreover, the extent of compromise is clearly dependent on the chemical structure, largely to the extent that the permeation is stratum corneum controlled in the intact skin. Thus, methanol passed through the dermis 120 times faster than through the whole skin, while the factor for pentanol was only ~13. The risk of systemic toxicities arising from inadvertent or deliberate topical applications to broken skin is greatest with polar nonelectrolytes and salts with little capacity to breach the intact stratum corneum. Such factors should be generally evaluated for suspect agents that are to be applied to the skin (cosmetic, drug, and household product ingredients).

Since the lower alcohol homologs are not extensively membrane bound, their permeability coefficients are not altered by retention and can be further quantitatively analyzed. The value of 0.318 cm/hr for methanol through heat-separated dermis translates to a total diffusional resistance of 3.14 hr/cm (a reciprocal relationship). By a previous estimate, no more than 0.83 hr/cm of this value is attributable to boundary layers, leaving at least 2.31 hr/cm as the effective aqueous tissue resistance contributed by the dermis[7]. The dermal thickness measured by a micrometer is 350 μm, which is roughly equivalent to the thickness of the assumed boundary layers. Thus, centimeter for centimeter, the hairless mouse dermis is about three times more resistant to diffusion than water itself.

The resistance of the full-thickness skin to methanol was 385 hr/cm, and the summed boundary layer and aqueous tissue resistances were <1% of the total resistance encountered when the skin was intact. Results

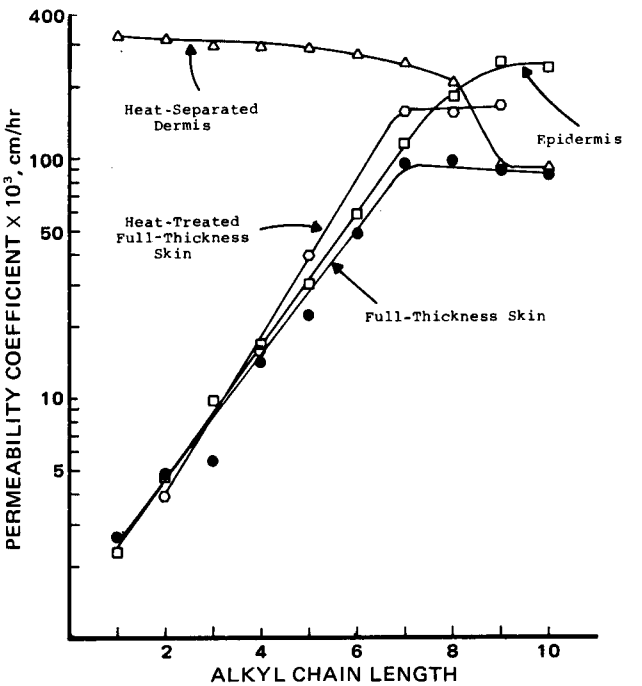

Figure 4—*Semilog plot of permeability coefficients for heat-processed hairless mouse membranes and normal hairless mouse skin as a function of alkyl chain length. All data were obtained at 37°.*

[7] Resistances in series are additive.

Table V—Permeability Coefficients ($P \times 10^3$, cm/hr [a]) of the Alkanols at 37° through Stripped Skin

Alkanol	Number of Strippings			
	5	10	15	25
Methanol	15.5	33.4 (38.2, 28.6)	—	313
Ethanol	14.1	32.1 (36.7, 27.5)	—	219
n-Propanol	13.0	22.2	130	218
n-Butanol	31.0	52.6 (45.2, 60.0)	157	215
n-Pentanol	47.5	79.6	—	217
n-Hexanol	—	—	—	209
n-Heptanol	—	—	—	223
n-Octanol	181[b]	197[b]	210[b]	225[b]
n-Nonanol	123[b]	126[b]	—	133[b]
n-Decanol	—	—	—	129[b]

[a] Except when indicated for 10 times stripping, the results represent single determinations. [b] These data may be affected by membrane retention and, therefore, represent apparent P values under the conditions of the experiment.

similarly obtained for other members of the homologous series are summarized in Table IV. The relative importance of the subepidermal layers rises rapidly with increasing alkyl chain length.

Data for the permeation of stripped skin are presented in Table V and are shown graphically in Fig. 5, which is a plot of log P_n *versus* alkyl chain length. The data are in full agreement with the previous analysis, with the following added features. As might be expected, as the stratum corneum was removed (thinned), the permeability coefficients of the lower homologs increased uniformly. However, the stripping apparently caused some pitting of the skin since the increases were disproportionate for methanol and ethanol.

The lower plateau formed for five and 10 strippings is characteristic of an aqueous pore route (12). When the entire stratum corneum is removed[8] (25 strippings), the profile appears to be qualitatively similar to

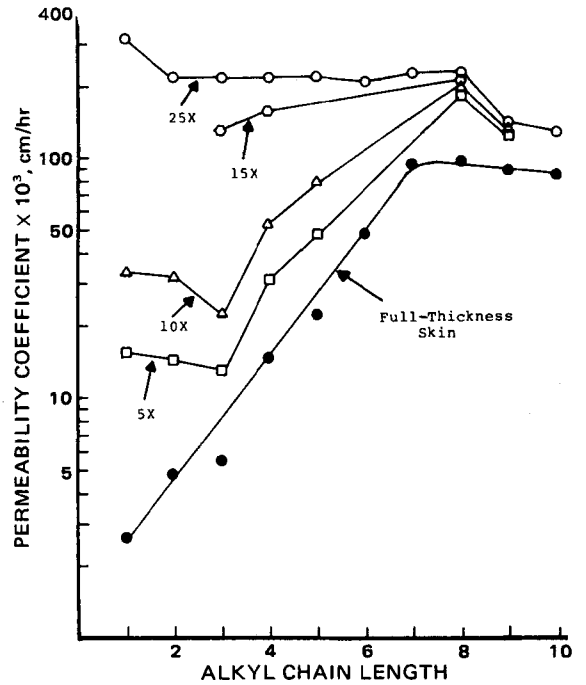

Figure 5—*Semilog plot of permeability coefficients for stripped hairless mouse membranes and normal hairless mouse skin as a function of alkyl chain length. All data were obtained at 37°. The skin was stripped 5, 10, 15, and 25 times.*

[8] Complete stripping was taken as the point where the surface became uniformly moist and glistening. The fact that this point represents essentially complete removal of the stratum corneum is indicated in the qualitative and quantitative parallels to heat-separated dermis.

that for heat-separated dermis. However, permeability coefficients are ~40% lower than those observed for heat-separated dermis. Several reasons can be advanced for this finding: incomplete removal of the stratum corneum so that the effective area for diffusion is somewhat reduced; the innate resistance of the viable epidermal layer, which is present with stripped skin but which is not a part of the heat-separated dermis; and damage to the dermis resulting from the heat-separation techniques. These aspects are under current laboratory investigation.

The present study further substantiates conclusions made previously (5) regarding a high degree of similarity between hairless mouse skin and human skin (17–19). Specifically, it is demonstrated that gross similarities seen histologically (20–22) translate to similarities in barrier properties. The cornified layer is the flux-determining feature for polar nonelectrolytes, and it acts as a lipid fabric in that oil–water partitioning into it is the principal determinant of the relative permeabilities of structurally similar compounds. When the stratum corneum is removed, the residual tissue offers little more than the resistance of a gelled aqueous phase to mass transfer, as was suggested by Scheuplein (18).

This study also showed how estimates of the effect of skin damage on the permeability of compounds may be roughly assessed by carefully fractionating the hairless mouse integument and determining the ratio of permeability of intact to broken skin. The more hydrophobic a compound, the closer this ratio will be to one, and, by extrapolation of the significance of the observation, the intrinsically safer the compound will be when applied to an irritated, diseased, or otherwise damaged skin surface, providing it is safe to use on intact skin in the first place.

REFERENCES

(1) W. Montagna and R. P. Parakkal, "The Structure and Function of Skin," 3rd ed., Academic, New York, N.Y., 1974.

(2) R. J. Scheuplein and I. H. Blank, *Physiol. Rev.*, **51**, 702 (1971).

(3) A. M. Kligman, in "The Epidermis," W. Montagna and W. C. Lobitz, Eds., Academic, New York, N.Y., 1964, chap. 20.

(4) B. Idson, *J. Soc. Cosmet. Chem.*, **22**, 615 (1971).

(5) H. Dürrheim, G. L. Flynn, W. I. Higuchi, and C. R. Behl, *J. Pharm. Sci.*, **69**, 781 (1980).

(6) R. Scheuplein, in "Physics and Pathophysiology of the Skin," vol. 5, A. Jarrett, Ed., Academic, New York, N.Y., 1978, pp. 1963–1730.

(7) A. S. Michaels, S. K. Chandrasekaran, and J. E. Schaw, *AIChE J.*, **21**, 985 (1975).

(8) G. L. Flynn and S. H. Yalkowsky, *J. Pharm. Sci.*, **61**, 838 (1972).

(9) R. G. Stehle and W. I. Higuchi, *ibid.*, **56**, 1367 (1967).

(10) S. S. Davis, T. Higuchi, and J. H. Rytting, *J. Pharm. Pharmacol.*, **24**, 30P (1972).

(11) S. S. Davis, T. Higuchi, and J. H. Rytting, *Adv. Pharm. Sci.*, **4**, 63 (1974).

(12) G. L. Flynn, S. H. Yalkowsky, and T. J. Roseman, *J. Pharm. Sci.*, **63**, 479 (1974).

(13) A. Leon, C. Hansch, and D. Elkins, *Chem. Rev.*, **71**, 525 (1971).

(14) C. Barnes, *Physics*, **5**, 4 (1934).

(15) J. L. Fox, G. L. Flynn, T. Hagen, W. I. Higuchi, N. F. H. Ho, and H. Dürrheim, "Abstracts," APhA Academy of Pharmaceutical Sciences, vol. 8 (2), Nov. 1978, p. 100.

(16) G. L. Flynn, C. R. Behl, T. Kurihara, W. Smith, J. Fox, H. Dürrheim, and W. I. Higuchi, "Abstracts," APhA Academy of Pharmaceutical Sciences, vol. 9 (1), 1979, p. 97.

(17) R. J. Scheuplein, *J. Invest. Dermatol.*, **45**, 334 (1966).

(18) *Ibid.*, **48**, 79 (1967).

(19) R. J. Scheuplein and I. H. Blank, *J. Invest. Dermatol.*, **60**, 286 (1975).

(20) W. D. Steward and J. O. Runikis, *ibid.*, **49**, 159 (1967).

(21) A. J. Aguiar and M. A. Weiner, *J. Pharm. Sci.*, **58**, 210 (1969).

(22) S. J. Mann, *J. Invest. Dermatol.*, **56**, 170 (1971).

ACKNOWLEDGMENTS

Presented at the Basic Pharmaceutics Section, APhA Academy of Pharmaceutical Sciences, New York meeting, May 1977 (Abstract 12).

Supported in part by National Institutes of Health Grant GM 24611.